ORIGINAL RESEARCH

Hypoxia-Inducible Factor-1α in SM22α-Expressing Cells Modulates Alveolarization

Elizabeth A. Barnes[1], Carsten Knutsen[1,2], Alida Kindt[3], Xibing Che[1], Lihua Ying[1], Eloa Adams[1], Erika Gonzalez[4], Prajakta Oak[4], Anne Hilgendorff[4], Cristina M. Alvira[1,2], and David N. Cornfield[1]

[1]Division of Pulmonary, Asthma, and Sleep Medicine, Center for Excellence in Pulmonary Biology, and [2]Division of Pediatric Critical Care Medicine, Department of Pediatrics, Stanford University School of Medicine, Stanford, California; [3]Metabolomics and Analytics Centre, Leiden Academic Centre for Drug Research, Leiden University, Leiden, the Netherlands; and [4]Comprehensive Pneumology Center, Ludwig Maximilian University of Munich, Munich, Germany

ORCID IDs: 0000-0002-9857-8657 (E.A.B.); 0000-0002-6921-0001 (C.M.A.); 0000-0002-1684-2056 (D.N.C.).

Abstract

Worldwide, the incidence of both preterm births and chronic lung disease of infancy, or bronchopulmonary dysplasia, remains high. Infants with bronchopulmonary dysplasia have larger and fewer alveoli, a lung pathology that can persist into adulthood. Although recent data point to a role for hypoxia-inducible factor-1α (HIF-1α) in mediating pulmonary angiogenesis and alveolarization, the cell-specific role of HIF-1α remains incompletely understood. Thus, we hypothesized that HIF-1α, in a distinct subset of mesenchymal cells, mediates postnatal alveolarization. To test the hypothesis, we generated mice with a cell-specific deletion of HIF-1α by crossing SM22α promoter–driven Cre mice with HIF-1α$^{flox/flox}$ mice (SM22α-HIF-1α$^{-/-}$), determined SM-22α–expressing cell identity using single-cell RNA sequencing, and interrogated samples from preterm infants. Deletion of HIF-1α in SM22α-expressing cells had no effect on lung structure at day 3 of life. However, at 8 days, there were fewer and larger alveoli, a difference that persisted into adulthood. Microvascular density, elastin organization, and peripheral branching of the lung vasculature were decreased in SM22α-HIF-1α$^{-/-}$ mice, compared with control mice. Single-cell RNA sequencing demonstrated that three mesenchymal cell subtypes express SM22α: myofibroblasts, airway smooth muscle cells, and vascular smooth muscle cells. Pulmonary vascular smooth muscle cells from SM22α-HIF-1α$^{-/-}$ mice had decreased angiopoietin-2 expression and, in coculture experiments, a diminished capacity to promote angiogenesis that was rescued by angiopoietin-2. Angiopoietin-2 expression in tracheal aspirates of preterm infants was inversely correlated with overall mechanical ventilation time, a marker of disease severity. We conclude that SM22α-specific HIF-1α expression drives peripheral angiogenesis and alveolarization in the lung, perhaps by promoting angiopoietin-2 expression.

Keywords: lung development; bronchopulmonary dysplasia; angiopoietin-2; oxygen sensing

In the initial description of bronchopulmonary dysplasia (BPD) by Northway and colleagues in 1967, postnatal lung injury was the result of exposure to high concentrations of inspired oxygen, aggressive positive pressure ventilation, or infection with inflammation (1, 2). As neonatal care has improved with therapeutic strategies that include prenatal steroid administration, surfactant replacement therapy, increasing use of noninvasive positive pressure ventilation, and low-volume ventilator strategy, the incidence of BPD in more mature (>28 wk) infants has decreased even as the overall incidence has increased, because of the survival of very low–birthweight infants. In infants of very low birthweight with BPD, the characteristic lung structure includes fewer and larger alveoli without inflammation, often termed "new BPD" (3).

Increasing incidence of new BPD highlights pulmonary endothelial cell (PEC) angiogenesis as a key determinant of alveolarization (3, 4). In infants with fatal BPD, proangiogenic factors are decreased, and pulmonary angiogenesis is impaired.

(Received in original form February 6, 2023; accepted in final form June 8, 2023)

Supported by NIH grants 1R01HD092316-01, HL-060784 (to D.N.C.), and HL-160018 (to D.N.C. and C.M.A.).

Author Contributions: E.A.B., A.K., E.G., P.O., L.Y., and E.A. performed experiments and analyzed data. C.K. analyzed data, contributed to study design, and assisted with manuscript preparation. X.C. performed experiments. E.A.B., A.H., C.M.A., and D.N.C. contributed to study design. A.H. provided patient samples. E.A.B. and D.N.C. prepared the manuscript.

Correspondence and requests for reprints should be addressed to David N. Cornfield, M.D., Division of Pulmonary, Asthma, and Sleep Medicine, Department of Pediatrics, Center for Excellence in Pulmonary Biology, Stanford University School of Medicine, 770 Welch Road, Stanford, CA 94305. E-mail: cornfield@stanford.edu.

This article has a related editorial.

This article has a data supplement, which is accessible from this issue's table of contents at www.atsjournals.org.

Am J Respir Cell Mol Biol Vol 69, Iss 4, pp 470–483, October 2023

Originally Published in Press as DOI: 10.1165/rcmb.2023-0045OC on June 8, 2023
Internet address: www.atsjournals.org

Clinical Relevance

In the present manuscript, we use a cell-specific strategy to delete hypoxia-inducible factor 1α (HIF-1α) protein in SM22α expressing cells. We used single cell transcriptomics to characterize the SM22α expressing cells. We found that, even in normoxia, loss of HIF-1α compromises postnatal alveolarization by decreasing angiogenesis, communication between specific mesenchymal cell populations and endothelial cells, and diminishing expression of angiopoietin-2. We provide data from human infants demonstrating an inverse relationship between disease severity and angiopoietin-2 expression. Taken together, we believe the work outlines a novel, cell-specific, and previously undescribed role for a HIF-1α in modulating alveolarization.

The structural and physiologic abnormalities evident in human BPD are mirrored by either pharmacologic or genetic inhibition of angiogenesis, which attenuates vascular growth and consequent alveolarization (5). In experimental models, the lung BPD phenotype can be rescued by the administration of exogenous vascular endothelial growth factor (VEGF), which preserves endothelial survival and function to mitigate hyperoxia-induced lung injury (6), a widely used preclinical model of BPD (4).

Hypoxia-inducible factors (HIFs), transcription factors that mediate the response to low-oxygen environments, promote angiogenesis in the postnatal lung by increasing the expression of proangiogenic molecules, including VEGF and angiopoietin-2 (ANG2) (7, 8). HIF-1α and HIF-2α may possess isoform- and cell-specific functions in the lung, given divergent expression patterns (9, 10). Modification in expression of either isoform can result in perinatal respiratory distress, severe cardiac and vascular malformations, or incomplete lung development (11, 12). In models of prematurity in both primate and ovine species, pulmonary HIF-1α and HIF-2α protein levels are markedly reduced, compared with levels in term counterparts (13, 14). HIF stabilization by manipulating prolyl hydroxylase activity either pharmacologically or by cell-specific genetic deletion confers protection to lung structure and growth, even in the presence of injurious stimuli (15, 16). Moreover, in the context of prenatal injury, HIF stabilization can mitigate the untoward sequelae of intrauterine inflammation on placental structure and postnatal lung growth (17). Taken together, these observations underscore the importance of gaining further insight into the isoform- and cell-specific role for HIFs in postnatal lung development.

We interrogated single-cell RNA-sequencing (scRNA-seq) data in mice at distinct developmental stages to determine the cell identity of SM22α-expressing cells. To gain further insight into the isoform- and cell-specific role of HIF in the neonatal lung, we generated mice with a deletion of HIF-1α in SM22α-expressing cells by crossing SM22α promoter–driven Cre recombinase mice with HIF-1α$^{flox/flox}$ and wild-type mice. To demonstrate clinical relevance, we interrogated tracheal aspirate fluid of human preterm infants. We determined that loss of HIF-1α from SM22α-expressing cells compromised angiogenesis and alveolarization, perhaps owing to cell-specific decreases in ANG2 production. Moreover, ANG2 expression in tracheal aspirate fluid was inversely proportional to disease severity in infants with BPD.

Methods

For a detailed description of the methods, *see* the data supplement.

Results

SM22α-Cell–Specific Deletion of HIF-1α in the Lung

In control mice, SM22α expression is present in the pulmonary arteries and airways at postnatal days 3 and 8 and in adults (Figure 1A). To determine the cell-specific role of HIF-1α, we constitutively deleted HIF-1α expression in SM22α-expressing cells by crossing mice expressing SM22α promoter–driven Cre recombinase with floxed HIF-1α mice (SM22α-HIF-1α$^{-/-}$). Cre recombinase activity is primarily present in the smooth muscle cells (SMCs) of the pulmonary arteries (PASMCs) in SM22α -HIF-1α$^{-/-}$ mice as detected by β-galactosidase expression (Figure 1B). HIF-1α expression is markedly decreased in the pulmonary arteries of SM22α-HIF-1α$^{-/-}$ mice, especially in SM22α-expressing cells, compared with controls (Figure 1C). To further confirm loss of HIF-1α expression in the target cells in SM22α-HIF-1α$^{-/-}$ mice, PASMCs were isolated from the pulmonary arteries of SM22α -HIF-1α mice and examined for HIF-1α protein expression. In PASMCs from SM22α -HIF-1α$^{-/-}$ mice, HIF-1α expression was absent, in contrast to the continued expression in SM22α-HIF-1α$^{+/+}$ mice (Figure 1D). To determine the specific cell populations affected by the SM22α-HIF-1α$^{-/-}$ genotype, scRNA-seq data of mesenchymal cells from the developing lung (18) were analyzed for *Tagln* (SM22α) and *Hif1α* expression (Figure 1E). Airway SMC, myofibroblast, and vascular SMC (VSMC) populations exhibited the highest expression of *Tagln*. VSMCs demonstrated the highest level of *Tagln* and *Hif-1α* coexpression, supporting the notion of cell-specific loss of Hif-1α. Taken together, these results confirm the constitutive loss of SMC HIF-1α in the pulmonary arteries of the SM22α-HIF-1α$^{-/-}$ mice.

HIF-1α Loss in SM22α-Expressing Cells Compromises Alveolarization

At 3 days, there was no difference in lung histology between SM22α-HIF-1α$^{-/-}$ mice and controls. However, at 8 days, the mean linear intercept was 54 ± 7% greater and radial alveolar count (RAC) was 28 ± 4% less in SM22α-HIF-1α$^{-/-}$ mice, compared with controls (Figures 2A and 2B). The compromise in alveolarization persisted into adulthood, as SM22α-HIF-1α$^{-/-}$ mice displayed a 53.5% increase in mean linear intercept and a 28.0% decrease in radial alveolar count, compared with controls.

Expression of elastin was disordered, but not quantitatively decreased, in adult SM22α-HIF-1α$^{-/-}$ mice, compared with controls (Figure 2C). At 8 days, both SM22α-HIF-1α$^{-/-}$ and SM22α-HIF-1α$^{+/+}$ mice expressed elastin generally (Figure 2C) and at the septal tips, consistent with the presence of myofibroblasts. Analysis of scRNA-seq data demonstrated that, after birth, multiple mesenchymal cell types expressed *Tagln* at high levels but that myofibroblasts are the predominant mesenchymal cell type coexpressing *Tagln* and *Pdgfra* (Figure 2D).

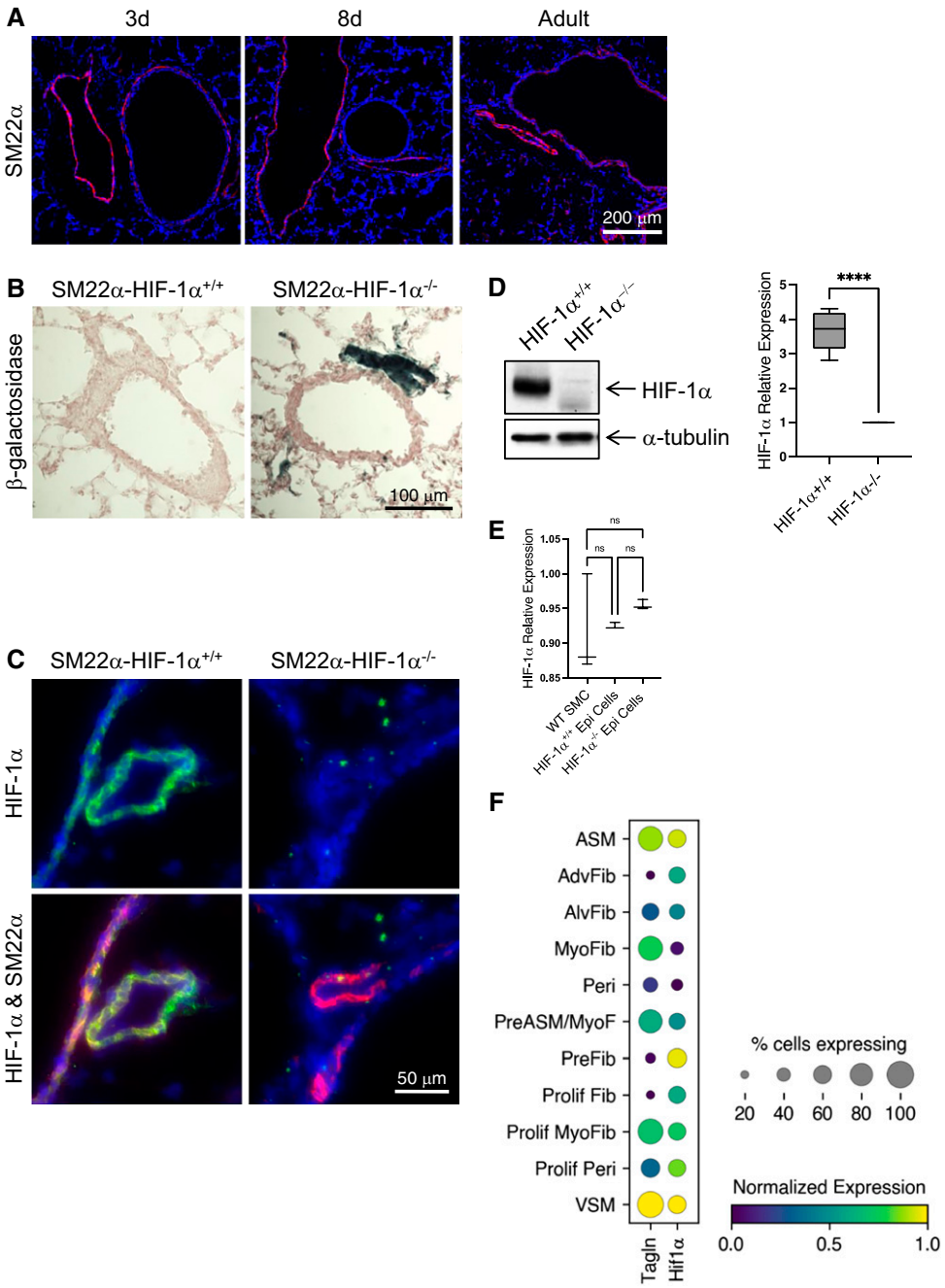

Figure 1. Deletion of smooth muscle cell (SMC) hypoxia-inducible factor 1α (HIF-1α) in SM22α-HIF-1α$^{-/-}$ mice. (*A*) Expression of SM22α protein in pulmonary arteries of SM22α-HIF-1α$^{+/+}$ mice (3 d, saccular stage; 8 d, alveolar stage; Adult, mature lungs). Red indicates SM22α, and blue indicates nuclei. Magnification, 100×. Scale bar, 200 μm. $n = 3$ per genotype. (*B*) β-galactosidase expression in pulmonary arteries from adult SM22α-HIF-1α mice. Blue indicates β-galactosidase, and red indicates Nuclear Fast Red counterstain. Magnification, 200×. Scale bar, 100 μm. $n = 3$ per genotype. (*C*) Expression of HIF-1α protein in pulmonary tissues of 3-day-old SM22α-HIF-1α mice. Red indicates SM22α, green indicates HIF-1α, and blue indicates nuclei. Magnification, 400×. Scale bar, 50 μm. $n = 3$ per genotype. (*D*) Expression of HIF-1α protein in isolated pulmonary artery SMCs (PASMCs) from SM22α-HIF-1α mice (HIF-1α$^{+/+}$ and HIF-1α$^{-/-}$ PASMCs) by western immunoblot. α-tubulin serves as a loading control. Data are shown as mean and range (minimum to maximum); ****$P < 0.0001$; $n = 6$ biological replicates (*E*) Expression of HIF-1α protein in isolated epithelil cells from SM22a mice (HIF-1$^{+/+}$ and HIF-1α$^{-/-}$ epithelial cells) by Western Immnoblot. E-cadherin serves as a control for epithelial cells and beta actin serves as a loading control. Data are shown as mean and range (minimum to maximum); $n = 3$ per genotype. (*F*) Dot plot showing level of expression (purple to yellow) and fraction of the population (dot size) expressing *Tagln* or *Hif1α* RNA from mesenchymal cell populations of the developing lung (E18.5, P1, P7, and P21) from wild-type mice (WT) as assessed by single-cell RNA sequencing (scRNA-seq) from GSE172251. Cell populations are abbreviated as follows: AdvFib = adventitial fibroblast; AlvFib = alveolar fibroblast; ASM = airway smooth muscle; Epi = epithelial; MyoFib = myofibroblast; ns = not significant; Peri = pericyte; PreASM/MyoF = myofibroblast and airway smooth muscle precursor; PreFib = fibroblast precursor; Prolif Fib = proliferating fibroblast; Prolif MyoFib = proliferating myofibroblast; Prolif Peri = proliferating pericyte; VSM = vascular smooth muscle; WT = wild-type.

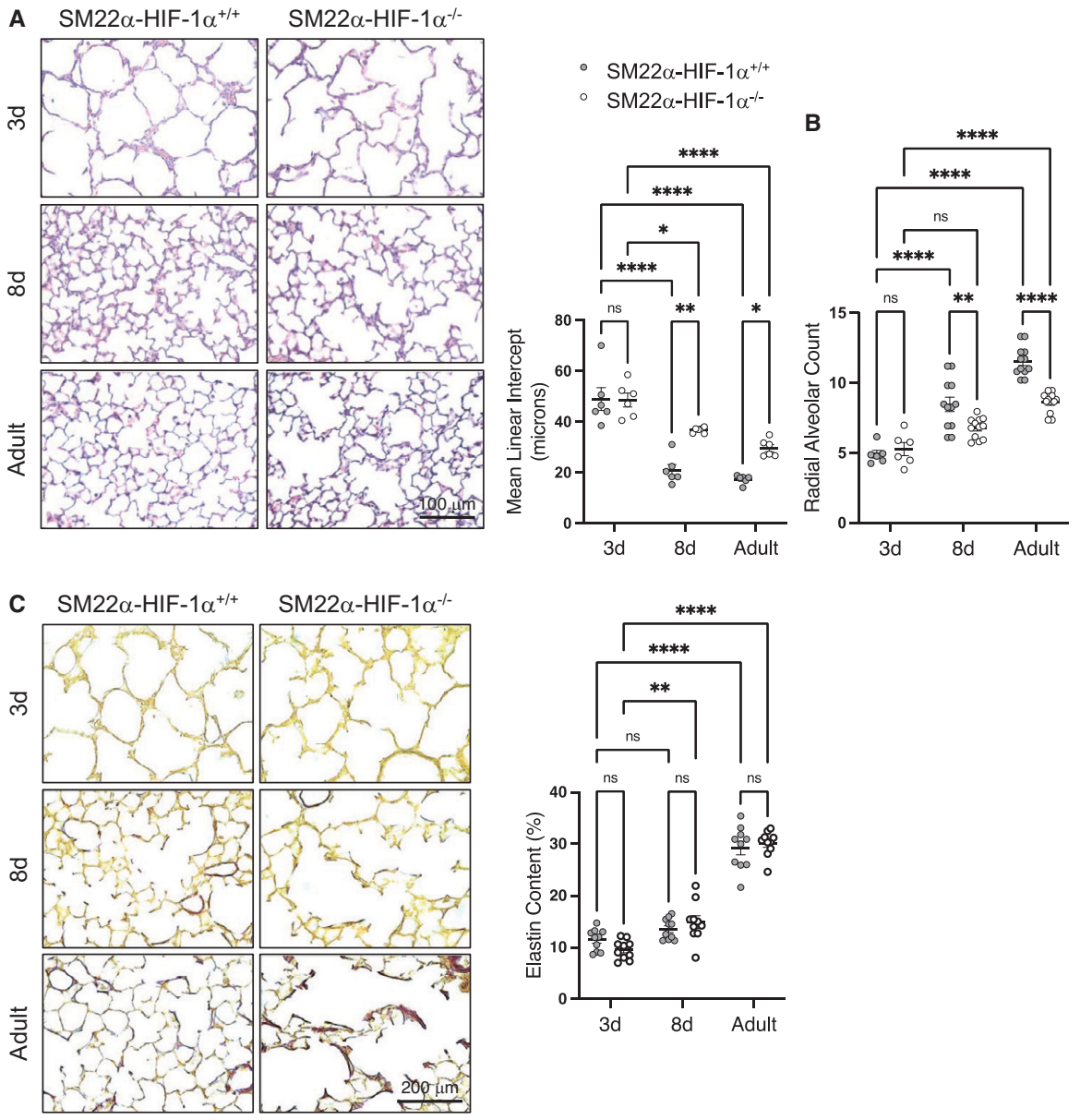

Figure 2. Loss of SM22α HIF-1α arrests alveolar development. (*A*) Hematoxylin and eosin (H&E)–stained images of lung parenchyma from SM22α-HIF-1α mice. Magnification, 200×. Scale bar, 100 μm. Mean linear intercept measurements for 3-day-old, 8-day-old, and adult SM22α-HIF-1α mice. Data are shown as mean ± SEM. *p ⩽ 0.05, **p ⩽ 0.01, ****p ⩽ 0.0001; *n* = 6 per genotype. (*B*) Radial alveolar count measurements for 3-day-old, 8-day-old, and adult SM22α-HIF-1α mice. Data are shown as mean ± SEM, ***P* <0.01, and *****P* <0.0001; *n* = 6-12 per genotype. (*C*) Elastin expression in lung tissues of SM22α-HIF-1α mice (3 d, saccular stage; 8 d, alveolar stage; adult, mature lungs). Brown indicates resorcin-fuchsin/Hart's elastic stain (elastin fibers), and yellow indicates counterstain. Magnification, 200×. Scale bar, 200 μm. Quantification of elastin content by ImageJ software analysis and represented as the amount of elastin content over total parenchyma content (%). Data are shown as mean ± SEM. ***P* < 0.01 and *****P* < 0.0001; *n* = 6-12 per genotype. (*D*) Heatmap of normalized expression of *Tagln* and *Pdgfra* mRNA from mesenchymal cell populations of the developing lung (P1 and P7) from WT mice as assessed by scRNA-seq. (*E*) Expression of SM22α protein in pulmonary tissues of SM22α-HIF-1α mice (3 d, saccular stage; 8 d, alveolar stage). Red indicates SM22α, and blue indicates nuclei. Magnification, 400×. Scale bar, 50 μm. (*F*) Expression of PDGFRα and α-smooth muscle cell actin (α-SMA) proteins in pulmonary tissues of SM22α-HIF-1α mice (3 d, saccular stage; 8 d, alveolar stage). Red indicates PDGFRα, green indicates α-SMA, and blue indicates nuclei. Magnification, 400×. Scale bar, 50 μm; *n* = 3 per genotype. Enlarged images are magnified at 1.67×-fold. Data are shown as mean ± SEM; ****p ⩽ 0.0001; *n* = 20 per group. HPF = high-powered field.

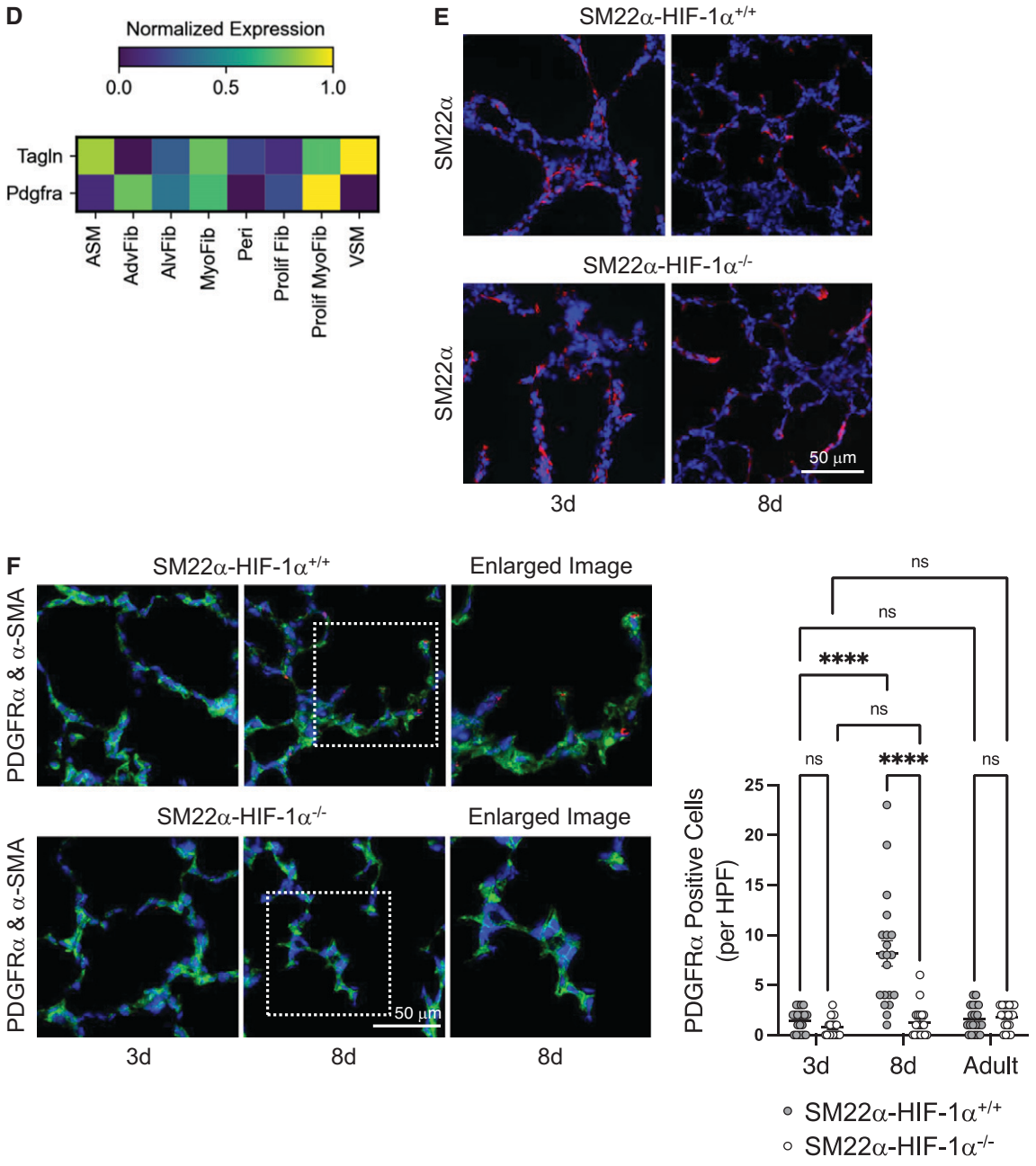

Figure 2. (*Continued*).

As shown in Figure 2E, at 8 days, both the SM22α-HIF-1α$^{+/+}$ and SM22α-HIF-1α$^{-/-}$ mice are positive for SM22α expression at the secondary alveolar septae, as detected by SM22α immunostaining. To further characterize the effect of SM22α-cell–specific loss of HIF-1α, PDGFRα expression was examined. In contrast to the SM22α-HIF-1α$^{+/+}$ mice, PDGFRα expression was absent in the septal tips of the SM22α-HIF-1α$^{-/-}$ mice (Figure 2F).

HIF-1α Loss in SM22α-Expressing Cells Compromises Pulmonary Angiogenesis

We next investigated whether pulmonary angiogenesis was compromised concomitant with impaired alveolarization. To approach the issue, lungs were stained for von Willebrand factor (VWF), an EC-specific molecule. At 8 days of life, there were markedly fewer von Willebrand factor–positive vessels of <150 μm in SM22α-HIF-1α$^{-/-}$ mice, compared with SM22α-HIF-1α$^{+/+}$ mice (Figure 3A). To assess the durability of the effect on the peripheral pulmonary vasculature, lungs from adult mice were injected with barium, and barium-injected arteries were quantified. There were significantly fewer barium-injected peripheral arterioles (<100 μm) in SM22α-HIF-1α$^{-/-}$ mice, compared with SM22α-HIF-1α$^{+/+}$ mice, both qualitatively and quantitatively (Figure 3B). This finding

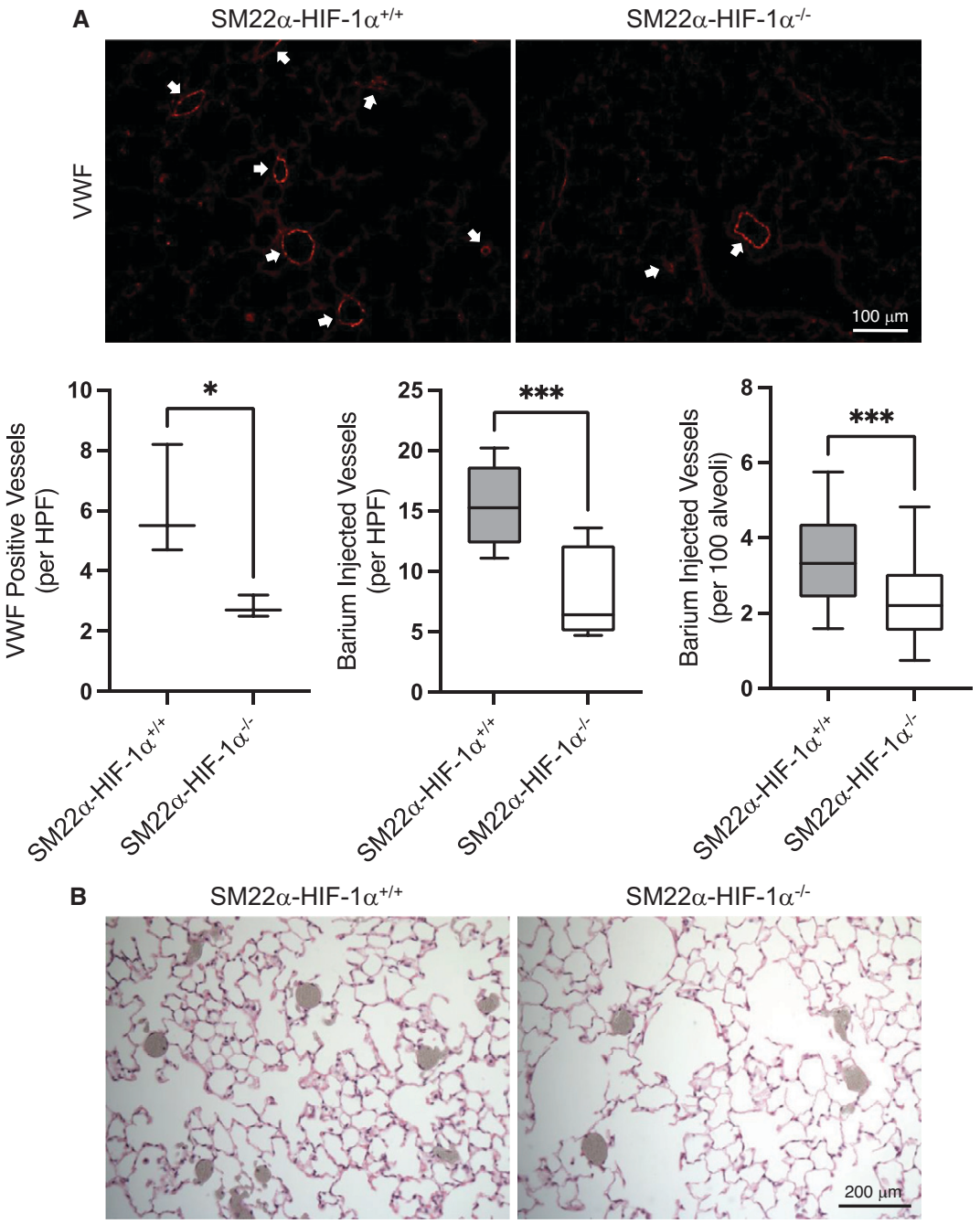

Figure 3. Loss of SM22α HIF-1α impairs pulmonary angiogenesis. (*A*) Expression of von Willebrand factor (VWF) in pulmonary tissues of 8-day-old SM22α-HIF-1α mice. Red indicates VWF. Magnification, 200×. Scale bar, 100 μm. As a measure of vascularity, VWF-positive vessels (≤150 μm) were counted per HPF. Data are shown as mean (minimum-maximum); *$P \leq 0.05$; $n = 3$ per genotype. (*B*) H&E–stained images of barium-injected lungs from adult SM22α-HIF-1α mice. Magnification, 100×. Scale bar, 200 μm. As a measure of vessel density, barium-filled distal arteries (≤100 μm) were counted per HPF and per 100 alveoli. Data are shown as mean (minimum-maximum); ***$p \leq 0.001$; $n = 4$-8 per genotype. (*C*) Three-dimensional images of α-SMA–stained vasculature from adult SM22α-HIF-1α mice. Left lobes were examined for the expression of α-SMA. Scale bars, 2.0 mm in the upper panels and 1.0 mm in the enlarged images in the lower panels. Quantification of bifurcated arteriole length (in millimeters) and number of branching arterioles (per artery) by ImageJ software analysis. Data are shown as mean (minimum-maximum); ****$p \leq 0.0001$; $n = 3$ per genotype. (*D*) Three-dimensional images of α-SMA–stained vasculature from adult SM22α-HIF-1α mice. Left lobes were examined. Scale bar, 0.5 mm. Quantification of distance between lung periphery and terminal arterioles (in millimeters) by ImageJ software analysis. Data are shown as mean (minimum-maximum); ***$P \leq 0.001$. (*E*) Quantification of left lobe area (in millimeters) and peripheral arteriole branch length (in millimeters) of adult SM22α-HIF-1α mice as assessed by ImageJ software analysis. Data are shown as mean (minimum-maximum); $n = 3$ per genotype.

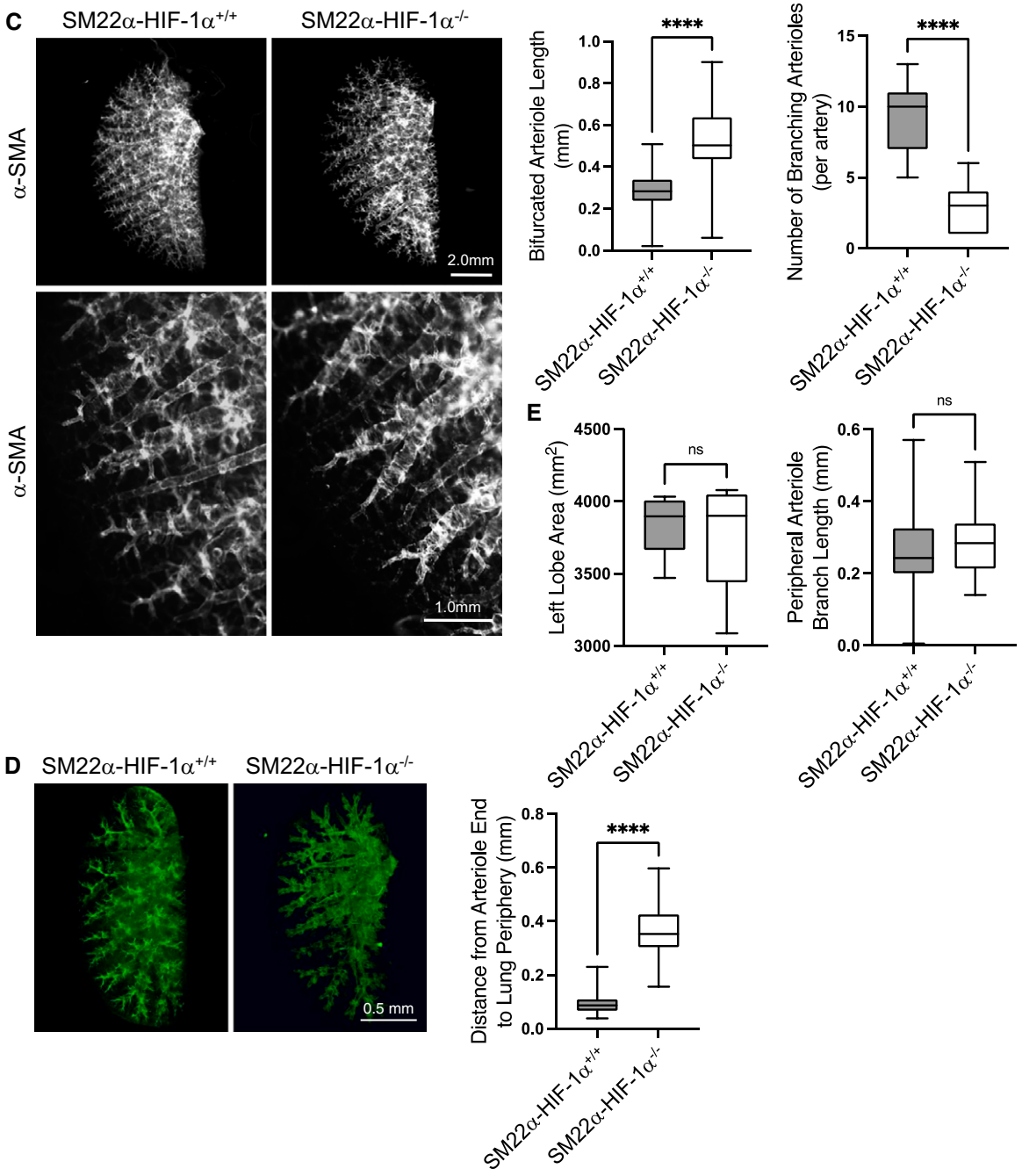

Figure 3. (*Continued*).

was further underscored by stereoscopic imaging and analysis of adult whole-lung tissues stained with α-smooth muscle actin (α-SMA) (Figure 3C). Qualitatively, there appears to be less vascular density in the SM22α-HIF-1α$^{-/-}$ mice, compared with SM22α-HIF-1α$^{+/+}$ mice (Figure 3C, top panels). Viewed at higher magnification, arterial branching occurs more proximally in SM22α-HIF-1α$^{-/-}$ mice, compared with SM22α-HIF-1α$^{+/+}$ mice (Figure 3C, bottom panels). There are fewer and longer arteriole branches in the arteries of SM22α-HIF-1α$^{-/-}$ mice relative to the SM22α-HIF-1α$^{+/+}$ mice. To further characterize this observation, stereoscopic images were pseudocolored to permit visualization of the lung periphery (Figure 3D). The distance between the lung periphery and terminal arterioles is increased for the SM22α-HIF-1α$^{-/-}$ mice, compared with SM22α-HIF-1α$^{+/+}$ mice, both qualitatively and quantitatively (Figure 3D). There was no difference in lung area between the two genotypes (Figure 3E).

HIF-1α Loss in SM22α-Expressing Cells Decreases ANG2 Expression

Given the central role for ECs in angiogenesis, we next focused on whether

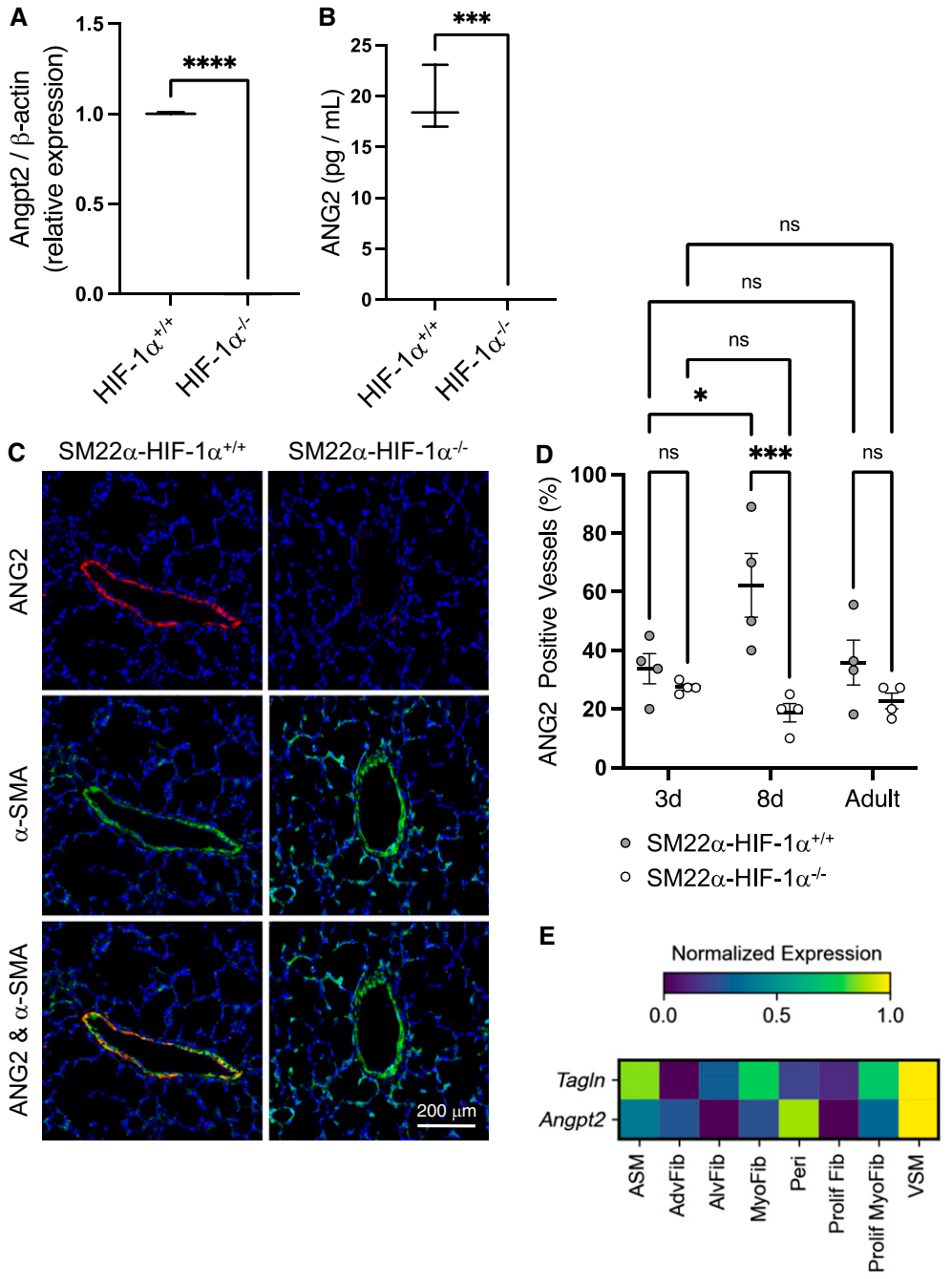

Figure 4. Loss of SMC HIF-1α decreases ANG2 expression. (*A*) Expression of *Angpt2* mRNA in isolated PASMCs from SM22α-HIF-1α mice (HIF-1α$^{+/+}$ and HIF-1α$^{-/-}$ PASMCs) by RT-qPCR. Data are shown as mean (minimum-maximum); ****p ⩽ 0.0001; $n = 3$ biological replicates. (*B*) Expression of secreted ANG2 protein in conditioned media from HIF-1α$^{+/+}$ and HIF-1α$^{-/-}$ PASMCs by ANG2 ELISA. Data are shown as mean (minimum-maximum); ***p ⩽ 0.001; n=3 biological replicates. (*C*) Images of ANG2 protein expression in pulmonary tissues of 8-day-old SM22α-HIF-1α mice. Red indicates ANG2, green indicates α-SMA, and blue indicates nuclei. Magnification, 200×. Scale bar, 200 μm. $n = 3$–6 per genotype. (*D*) Quantification of ANG2-positive vessels represented as the amount of ANG2-positive vessels over total vessels counted (%). Data are shown as mean ± SEM. *P ⩽ 0.05, and ***P ⩽ 0.001. (*E*) Heatmap of normalized expression of *Tagln* and *Angpt2* mRNA from mesenchymal cell populations of the developing lung (P1 and P7) from WT mice as assessed by scRNA-seq.

factors secreted from SM22α-expressing cells might be altered by the deletion of HIF-1α. Thus, we interrogated whether the deletion of HIF-1α in SM22α-expressing cells alters expression of the HIF-1α targets VEGF (19) and ANG2 (20). PASMCs from SM22α-HIF-1α$^{+/+}$ mice, but not SM22α-HIF-1α$^{-/-}$ mice, expressed both *Vegf* and *Angpt2* (Figure 4A). The conditioned media from SM22α-HIF-1α$^{+/+}$ mice, but not SM22α-HIF-1α$^{-/-}$ mice, expressed ANG2 (Figure 4B). These findings were further

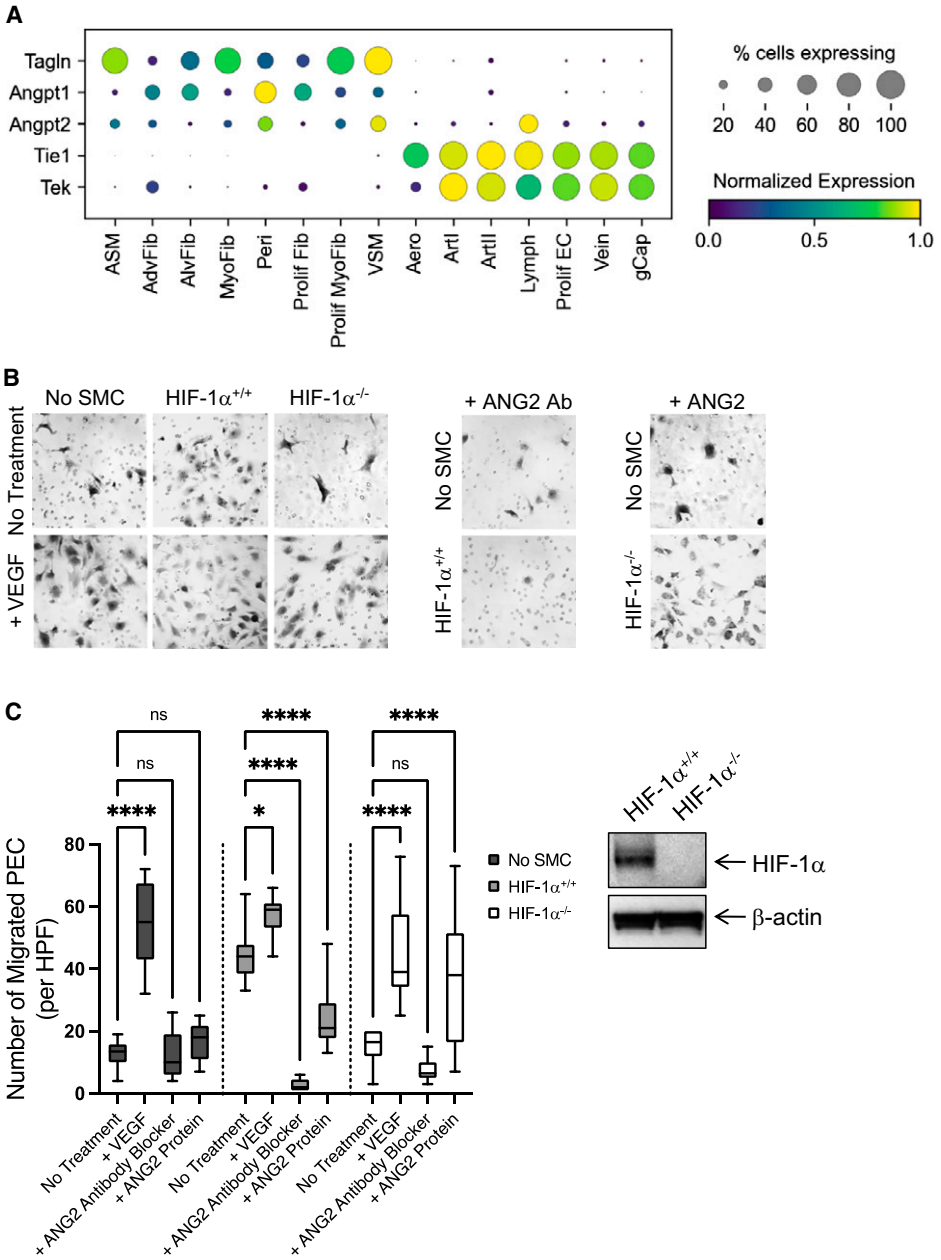

Figure 5. Loss of SMC HIF-1α inhibits endothelial cell (EC) migration and EC-driven angiogenesis. (*A*) Dot plot showing level of expression (purple to yellow) and fraction of the population (dot size) expressing mRNA of gene products involved in angiopoietin signaling from mesenchymal cell and EC populations of the postbirth developing lung (P1 and P7) from WT mice as assessed by scRNA-seq from GSE172251 and GSE159804, respectively. Cell populations are abbreviated as follows: ASM, AdvFib, AlvFib, MyoFib, Peri, Prolif Fib, Prolif MyoFib, VSM, arterial EC I (ArtI), arterial EC II (ArtII), Car4+ capillaries (Aero), lymphatic EC (Lymph), proliferative EC (Pro EC), venous EC (Vein), Car4− capillaries (gCap). (*B*) Migration of murine pulmonary ECs (PECs) using a modified Boyden chamber assay. Isolated HIF-1$\alpha^{+/+}$ and HIF-1$\alpha^{-/-}$ PASMCs were seeded in the bottom well with PECs seeded in the top chamber. Samples were treated with or without vascular endothelial growth factor (VEGF), angiopoietin-2 antibody (ANG2 Ab), or angiopoietin 2 protein (ANG2). Representative images are shown; magnification 200×; $n = 4$ biological replicates. (*C*) The number of migrated PECs (per HPF) after 24 hours was assessed. Data are shown as mean (minimum-maximum); *p ⩽ 0.05, ****p ⩽ 0.0001. Expression of HIF-1α protein in isolated PASMCs from SM22α-HIF-1α mice (HIF-1$\alpha^{+/+}$ and HIF-1$\alpha^{-/-}$ PASMCs) by western immunoblot. β-actin serves as a loading control. (*D*) Angiogenesis driven by murine PECs using a Growth Factor Reduced BD Matrigel angiogenesis assay. 100,000 murine PECs were incubated with 100,000 HIF-1$\alpha^{+/+}$ PASMCs, with HIF-1$\alpha^{-/-}$ PASMCs, or alone for 5 days. Samples were treated with or without VEGF, ANG2 Ab, or ANG2. Magnification 200×. Scale bar, 100 μm; $n = 3$ biological replicates. (*E*) VE-cadherin stained angiogenic networks using a GFR BD Matrigel angiogenesis assay. (*F*) Angiogenesis assay with 10,000 murine PECs incubated with 100,000 HIF-1$\alpha^{+/+}$ PASMCs or HIF-1$\alpha^{-/-}$ PASMCs for 3 days. Samples were treated with or without ANG2 Ab or ANG2. Magnification, 400×. Scale bar, 50 μm; $n = 3$ biological replicates. As a measure of angiogenesis, tube length (in microns) and the number of tubes formed (per cell colony) were assessed. Data are shown as mean ± SEM; ****p ⩽ 0.0001 and as mean (minimum-maximum); ***p ⩽ 0.001, ****p ⩽ 0.0001, respectively.

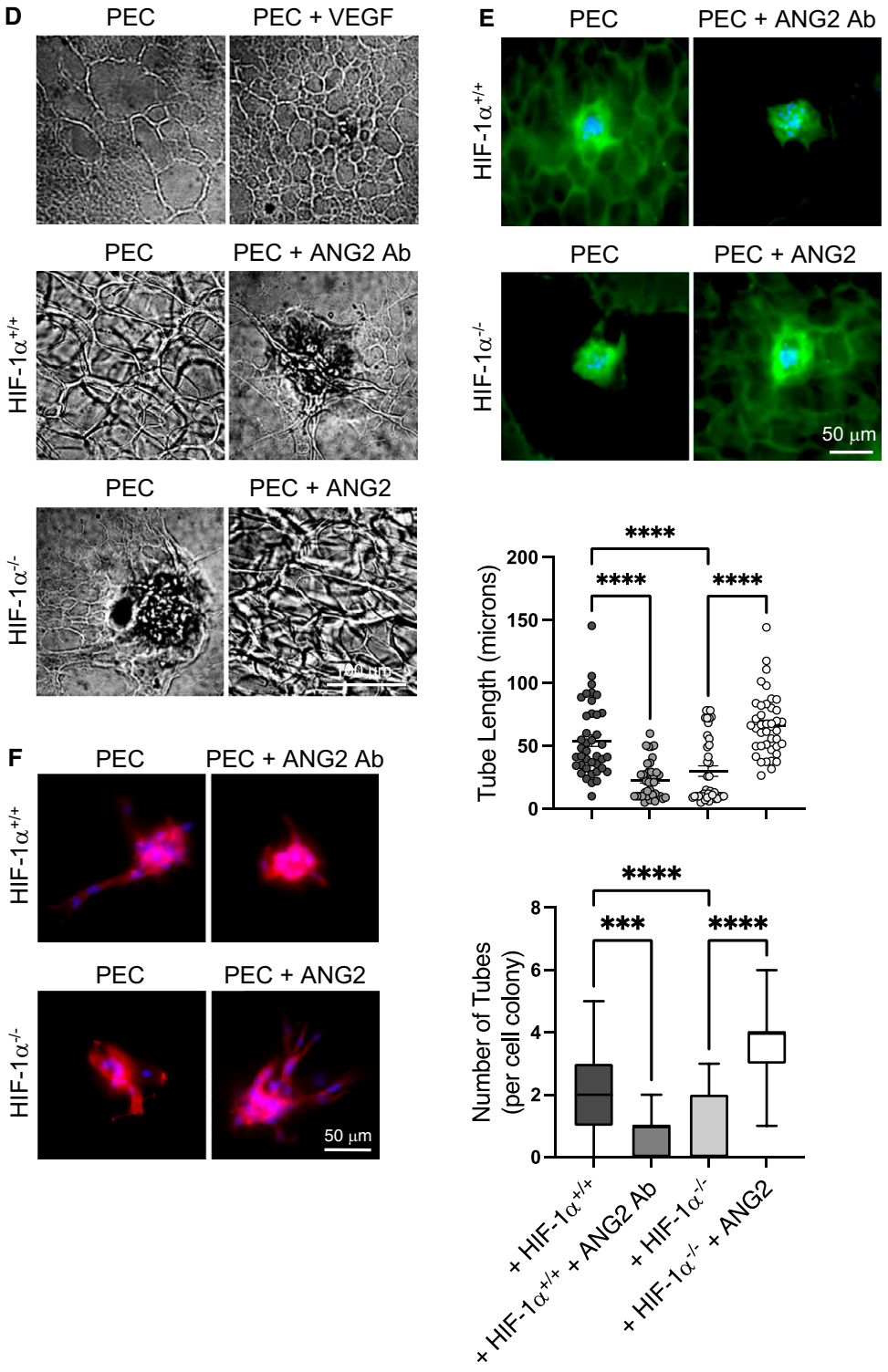

Figure 5. (*Continued*).

confirmed with immunohistochemistry on lung tissue from 8-day-old mice wherein ANG2 expression (indicated in red) was present in lungs from SM22α-HIF-1α$^{+/+}$ mice but not those from SM22α-HIF-1α$^{-/-}$ mice (Figure 4C, upper panels). Staining for α-SMA demonstrated ANG2 in α-SMA–expressing cells (Figure 4C, lower panels). Quantification of ANG2-positive vessels demonstrated that the frequency of ANG2-expressing vessels was greatest at 8 days, coincident with early alveolarization,

Table 1. Patient Information

ID	Preeclampsia	Gender	Age, wk	Birth Weight, g	MV. d	O_2, d	FIO_2, Day 28	Sample	
								Day of Life	FIO_2
Mbac481	No	F	23.57	590	70	142	0.40–0.70	31	0.35
Mljt258	No	M	25.00	680	60	68	0.25–0.40	7	0.50
Mzjr061	No	M	25.00	760	62	73	0.38–0.59	7	0.26
Myme912	No	M	26.14	925	45	93	0.24–0.50	12	0.27
Mdlv347	No	M	25.43	780	67	63	0.26–0.35	7	0.29
Mwsz573	No	M	25.29	740	55	108	0.27–0.42	28	0.22
Mvfk822	No	F	24.14	650	53	89	0.26–0.60	12	0.30
M081zsh	No	M	25.43	730	78	123	0.74–1.00	10	0.30
M290afj	No	M	23.57	530	56	85	0.55	14	0.49
M951afc	No	F	26.71	890	43	103	0.31–0.39	9	0.26
M858mgx	N/A	M	25.57	970	57	64	0.29–0.40	13	0.53
Myly782*	Yes	M	30.43	930	3	1	0.21	8	0.21
Mrez567*	Yes	M	30.14	1370	11	8	0.21	8	0.21

Definition of abbreviations: BPD = bronchopulmonary dysplasia; F = female; FIO_2 = fraction of inspired oxygen; M = male; MV = minute ventilation; N/A = not applicable.
ELISA for angiopoietin-2 from tracheal aspirates during the first week of life.
Log_2-transformed expression data corrected for gestational age and early onset of infection.
Wilcoxon and *t* tests performed to identify significance for BPD grades (0/1 versus 2/3).
Regression analysis was performed to identify significance for mechanical ventilation with oxygen supplementation (days) and O_2 supplementation (days).
Analyses included all infants presented in the table. Exception: analysis for "overall days of mechanical ventilation" and "overall days of oxygen supplementation" were repeated for only those infants with BPD grades 1, 2, and 3 (results displayed).
*Denotes patients without BPD.

a stage of lung development marked by profound angiogenesis. At 8 days, there were significantly fewer ANG2-expressing vessels in the lungs of SM22α-HIF-1α$^{-/-}$ mice, compared with SM22α-HIF-1α$^{+/+}$ mice (Figure 4D). Analysis of scRNA-seq data demonstrated that VSMCs are the cell population that most prominently express both *Tagln* and *Angpt2* (Figure 4E), providing further evidence that compromised *Angpt2* in the SM22α-HIF-1α$^{-/-}$ mice derives from the loss of PASMC HIF-1α expression.

HIF-1α Loss in SM22α-Expressing Cells Compromises EC Migration

Analysis of scRNA-seq data from pulmonary mesenchymal cells and ECs revealed that the VSMC population expresses a high level of *Angpt2* and that the EC populations highly express the receptors for ANG2, *Tie1*, and *Tek*, suggesting crosstalk between SMCs and the multiple EC subtypes (Figure 5A). To further detail the mechanism whereby loss of PASMC HIF-1α affects pulmonary angiogenesis, we interrogated whether PASMCs provide a promigratory signal

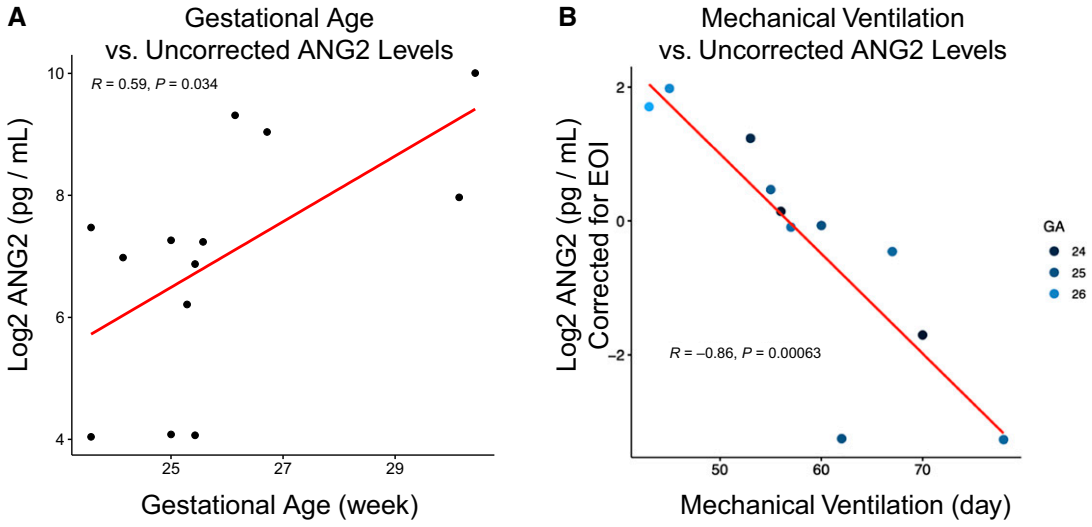

Figure 6. Tracheal aspirate ANG2 increases with gestation and is inversely proportional to BPD severity. (*A*) Tracheal aspirate samples from preterm infants were examined for the expression of ANG2 protein by ANG2 ELISA. Graph represents the positive correlation between ANG2 expression and gestational age (GA) in weeks. $P = 0.034$. (*B*) Significant negative correlation of ANG2 expression levels (log2 transformed; $R = 0.86$, $p = 0.00063$) with the duration of mechanical ventilation (day) in preterm infants with BPD. The analysis is corrected for the presence of early onset of infection (EOI). Shades of blue indicate groups of gestational age (week). Red line is the best-fit line.

to ECs. PASMCs were seeded in the bottom well, and PECs were seeded in the upper chamber. PEC migration was significantly greater in the presence of HIF-1α$^{+/+}$ PASMCs than in the presence of HIF-1α$^{-/-}$ PASMCs (Figure 5B). VEGF increased PEC migration in all conditions. Soluble ANG2 antibody blocked PEC migration to HIF-1α$^{+/+}$ PASMCs, whereas ANG2 significantly increased PEC migration to HIF-1α$^{-/-}$ PASMCs (Figure 5C). Immunoblotting of isolated PASMCs confirmed that HIF-1α protein is expressed in HIF-1α$^{+/+}$, but not HIF-1α$^{-/-}$, PASMCs.

To determine whether loss of PASMC HIF-1α affects angiogenesis (Figure 5D), PECs were grown on Growth Factor Reduced Matrigel (Corning), in the presence and absence of PASMCs, for 5 days. PECs alone generated a two-dimensional vascular network. The addition of VEGF to PECs increased the complexity of the tubes formed. In coculture studies, HIF-1α$^{+/+}$ PASMCs and PECs further increased complexity. The addition of ANG2 antibody to cocultures that included HIF-1α$^{+/+}$ PASMCs and PECs blocked the increase. Consistent with the EC migration studies, cocultures with HIF-1α$^{-/-}$ PASMCs and PECs did not increase complexity above PECs alone with a large number of cells surrounded by a limited concentric vascular network. Addition of ANG2 protein to cocultures of HIF-1α$^{-/-}$ PASMCs and PECs markedly increased complexity (Figure 5D).

To quantify the effect of PASMC HIF-1α expression on PEC tube formation, the Growth Factor Reduced Matrigel assays were modified (Figures 5E and 5F) to include a reduced number of PECs (10%). After 3 days, cells were stained for f-actin expression to visualize SMCs and ECs. Coculture of HIF-1α$^{+/+}$ PASMCs and PECs generated cell colonies with tubal outgrowths. The addition of ANG2 antibody blocked the increase in tube number and length. In coculture experiments with HIF-1α$^{-/-}$ PASMCs and PECs, tube formation and length were limited; however, the addition of ANG2 markedly increased the number and length of tubes formed.

ANG2 Expression Increases with Gestation and Is Decreased in Infants with BPD

To address whether ANG2 might play a role in the development of BPD in preterm human infants, tracheal aspirates from 13 preterm infants were examined for ANG2 expression (Table 1). It is interesting that gestational age correlated positively with ANG2 levels in tracheal aspirates, with a progressive increase between 24 and 30 weeks of gestational age (Figure 6A). Eleven of the 13 preterm infants developed BPD and were mechanically ventilated. Among the mechanically ventilated infants, ANG2 levels correlated inversely with duration of mechanical ventilation (Figure 6B). Given that duration of mechanical ventilation can be considered a proxy for BPD severity, lower levels of ANG2 might possess prognostic implications for infants with severe BPD.

Discussion

Lung development is carefully orchestrated, requiring temporally and spatially specific molecular expression. To determine the cell-specific role of the transcription factor HIF-1α in neonatal lung development, the molecule was deleted from SM22α-expressing cells. This strategy resulted in the loss of HIF-1α in SM22α-expressing cells. The present data argue that HIF-1α plays a previously unknown cell-specific and temporally specific role in mediating alveolarization. Although loss of HIF-1α in SM22α-expressing cells had no effect on lung structure through the saccular stage, lung alveolarization was attenuated by 8 days, an effect that persisted through adulthood. The decrease in overall and peripheral pulmonary vascular density corresponded with a marked decrease in ANG2 expression in the pulmonary vasculature, an observation buttressed by scRNA-seq data demonstrating that VSMCs in the developing lung normally express *Angpt2*. Coculture experiments further underscored the importance of HIF-1α expression in VSMCs in facilitating EC migration and angiogenesis. Data from preterm human infants, wherein BPD severity is inversely proportional to ANG2 levels in tracheal aspirates, represents further proof of concept. Given that BPD most significantly affects alveolarization, these data provide insight into the molecular pathogenesis of a disease, BPD, of indeterminate clinical cause and uncertain natural history. These observations demonstrate a temporally specific, proangiogenic role for HIF-1α in SM22α-expressing cells that promotes alveolarization, even in normoxia.

In the lung, the expression patterns of HIF-1α and HIF-2α are relatively distinct, arguing for functions that are both cell type and isoform specific (21). Data from genetic models offer further support for this construct as deletion of HIF-1α is embryonically lethal (22), whereas loss of HIF-2α leads to ∼50% embryonic death, with neonatal respiratory distress and death in surviving pups (23). Pharmacologic stabilization of HIF by means of nonspecific prolyl hydroxylase activity inhibition preserves lung structure and function, despite injurious stimuli such as mechanical ventilation (15), hyperoxia (24), or intrauterine inflammation (17). Moreover, HIF-1α stabilization in SM22α-expressing cells protects the neonatal lung from hyperoxia-induced injury, an observation that buttresses the present findings (16). The contrast between the present findings and the report wherein HIF-1α stabilization in the pulmonary epithelium compromised branching morphogenesis, lung maturation, and increased pulmonary hemorrhage highlights the importance of both cell type– and isoform-specific knowledge (25). For example, in the adult lung, pulmonary artery EC HIF stabilization results in vascular remodeling and pulmonary hypertension owing to increased HIF-2α, and not HIF-1α (26, 27). The present results are the first to outline an SM22α-expressing cell type–specific role for HIF-1α in mediating alveolarization.

Even absent HIF-1α in SM22α-expressing cells, lung development occurs without evident compromise through the saccular phase, the vast majority of which occurs in the relatively hypoxic intrauterine environment (28). Lung structure was affected only during early alveolarization, which, in both humans and mice, occurs in a relatively oxygen-rich environment (29), underscoring a role for HIF-1α, even in normoxia. Prior work has also pointed to a cell-specific, normoxic role for HIF-1α in maintaining low pulmonary vascular resistance (30). The importance of HIF-1α in SM22α-expressing cells in a normoxic environment, in contrast to the intrauterine environment, may relate to regional hypoxia as a driver of angiogenesis (31), a critical determinant of alveolarization. Consistent with this notion, the effects on lung development were differentially distributed to the periphery, regions that were most likely to be hypoxic. Arteriole branches originated and terminated relatively more

proximally in mice lacking HIF-1α in SM22α-expressing cells, pointing to a non–cell-autonomous role for HIF-1α in pulmonary angiogenesis that drives alveolarization. The relatively diminished vascular density and decreased alveolar number in the present model—the results of loss of HIF-1α in SM22α-expressing cells—are entirely consistent with the findings in human infants with BPD (5, 32). These observations suggest that local hypoxia in the peripheral lung during physiologic development might lead to HIF-1α stabilization in lung mesenchymal cells to increase ANG2 production and augment EC migration and angiogenesis.

Although the present approach entails HIF-1α deletion specifically in SM22α-expressing cells, scRNA-seq data underscore the potential involvement of multiple cell types. *Tagln*, which encodes SM22α, is well expressed in multiple mesenchymal cell types, including myofibroblasts, airway SMCs, and VSMCs. Among these *Tagln*-expressing cell types, HIF-1α is most well expressed in VSMCs. Myofibroblasts, cells critical for secondary septation (33) of the lung and elastin deposition (34), express *Tagln* and HIF-1α. The disordered elastin expression and decreased secondary septation and PDGFRα expression at the septal tips in mice with HIF-1α deletion in SM22α-expressing cells implicate a role for myofibroblasts. The notion that HIF-1α and PDGFRα expression are correlated has a precedent, as in both hepatocellular carcinoma (35) and glioblastoma (36) *Hif1α* and *Pdgfra* gene expression are positively correlated. Whether HIF-1α expression directly or indirectly affects PDGFRA expression merits further investigation.

Findings from human infants offer support, albeit indirect, for a construct wherein cell-specific HIF-1α–driven ANG2 production increases secondary septation of the lung. Consistent with prior reports, tracheal aspirate ANG2 expression correlated directly with gestational age. ANG2 expression levels increased significantly during the saccular phase of lung development, mirroring findings during murine lung development (37). Moreover, among the 11 of the 13 infants sampled who did develop BPD, the duration of mechanical ventilatory support correlated inversely with ANG2 levels in the tracheal aspirates. The timing of the sample collection, as well as the correlative design of the study, does not eliminate the potential that the increases in ANG2 levels might result from inflammation associated with infection, high concentrations of inspired oxygen, or ventilator-associated lung injury (38). Although prior reports argue that elevation of ANG2 in tracheal aspirates represents an unfavorable prognostic sign (39), the present data address disease severity as opposed to the presence or absence of BPD. Given that ANG2 can stimulate EC migration and sprouting with inhibition impairing sprouting tip migration (40), a context-specific, proangiogenic role for ANG2 is not unexpected in the neonatal lung. The findings from *in vitro* experiments wherein ANG2 rescued endothelial migration in coculture experiments with HIF-1α$^{-/-}$ PASMCs offer further support for this construct.

Taken together, the present findings outline a proangiogenic role for ANG2. Whereas angiopoietin-1 is an agonist for Tyr kinase with immunoglobulin and epidermal growth factor homology domains (Tie2), ANG2 is a context-dependent antagonist that can inhibit ANG1-induced Tie2 phosphorylation (41). In the neonatal lung, the role of ANG2 may be more complex than prior reports (39) suggest and possess context-specific effects (42). When ANG2 receptor binding occurs in the presence of VEGF, conditions favor angiogenesis, as endothelial junctional integrity and pericyte-EC interactions decrease and EC migration, vascular sprouting, and proliferation increase. Conversely, absent VEGF, ANG2 can cause EC apoptosis (43). In disease states such as BPD, when VEGF expression is decreased but not absent, whether ANG2 plays a predominately pro- or antiangiogenic role remains unknown.

Limitations of the present study include use of a genetic loss-of-function strategy using a Cre recombinase driven by a promoter, *Tagln*, that is expressed in several cell subtypes in the mesenchyme (44). Use of an inducible Cre with a *Notch3* driver might reveal greater detail surrounding the loss of the HIF-1a deletion in VSMCs and pericytes at specific developmental time points (45). Moreover, in the present report, only a single HIF isoform was deleted. Although significant amounts of HIF-2α protein were not noted in the cells of interest, the effects of any residual HIF-2α may have been disproportionately significant. The present findings would be further strengthened by *in vivo* experiments demonstrating that alterations in ANG2 expression, either in specific cell types or even more generally, can modulate alveolarization.

Overall, the present work demonstrates a cell-specific role for HIF-1α in SM22α-expressing cells in the lung at a temporally specific point in development. We report a non–cell-autonomous effect of HIF-1α expression in SM22α cells to promote endothelial migration, distal pulmonary vascular development, elastin organization, and secondary septation of the lung, perhaps because of increases in the expression of downstream targets of HIF, ANG2, and VEGF. These results highlight the importance of cell-type– and isoform-specific insight into HIF, especially early in air-breathing life, when angiogenesis drives a logarithmic increase in alveolar number (2–6). ■

Author disclosures are available with the text of this article at www.atsjournals.org.

Acknowledgment: The authors thank R. Metzger, Ph.D., for reagents and protocols and C. Chen for technical assistance.

References

1. Northway WH Jr, Rosan RC, Porter DY. Pulmonary disease following respirator therapy of hyaline-membrane disease. Bronchopulmonary dysplasia. *N Engl J Med* 1967;276:357–368.
2. Hilgendorff A, Reiss I, Ehrhardt H, Eickelberg O, Alvira CM. Chronic lung disease in the preterm infant. Lessons learned from animal models. *Am J Respir Cell Mol Biol* 2014;50:233–245.
3. Abman SH. Bronchopulmonary dysplasia: "a vascular hypothesis". *Am J Respir Crit Care Med* 2001;164:1755–1756.
4. Alvira CM, Morty RE. Can we understand the pathobiology of bronchopulmonary dysplasia? *J Pediatr* 2017;190:27–37.
5. Jakkula M, Le Cras TD, Gebb S, Hirth KP, Tuder RM, Voelkel NF, *et al.* Inhibition of angiogenesis decreases alveolarization in the developing rat lung. *Am J Physiol Lung Cell Mol Physiol* 2000;279:L600–L607.
6. Thébaud B, Ladha F, Michelakis ED, Sawicka M, Thurston G, Eaton F, *et al.* Vascular endothelial growth factor gene therapy increases survival, promotes lung angiogenesis, and prevents alveolar damage in hyperoxia-induced lung injury: evidence that angiogenesis participates in alveolarization. *Circulation* 2005;112:2477–2486.

7. Asikainen TM, Schneider BK, Waleh NS, Clyman RI, Ho WB, Flippin LA, *et al.* Activation of hypoxia-inducible factors in hyperoxia through prolyl 4-hydroxylase blockade in cells and explants of primate lung. *Proc Natl Acad Sci USA* 2005;102:10212–10217.
8. Milkiewicz M, Pugh CW, Egginton S. Inhibition of endogenous HIF inactivation induces angiogenesis in ischaemic skeletal muscles of mice. *J Physiol* 2004;560:21–26.
9. Tibboel J, Groenman FA, Selvaratnam J, Wang J, Tseu I, Huang Z, *et al.* Hypoxia-inducible factor-1 stimulates postnatal lung development but does not prevent O_2-induced alveolar injury. *Am J Respir Cell Mol Biol* 2015;52:448–458.
10. Tang H, Babicheva A, McDermott KM, Gu Y, Ayon RJ, Song S, *et al.* Endothelial HIF-2α contributes to severe pulmonary hypertension due to endothelial-to-mesenchymal transition. *Am J Physiol Lung Cell Mol Physiol* 2018;314:L256–L275.
11. Kotch LE, Iyer NV, Laughner E, Semenza GL. Defective vascularization of HIF-1α-null embryos is not associated with VEGF deficiency but with mesenchymal cell death. *Dev Biol* 1999;209:254–267.
12. Compernolle V, Brusselmans K, Acker T, Hoet P, Tjwa M, Beck H, *et al.* Loss of HIF-2α and inhibition of VEGF impair fetal lung maturation, whereas treatment with VEGF prevents fatal respiratory distress in premature mice. *Nat Med* 2002;8:702–710.
13. Asikainen TM, Ahmad A, Schneider BK, White CW. Effect of preterm birth on hypoxia-inducible factors and vascular endothelial growth factor in primate lungs. *Pediatr Pulmonol* 2005;40:538–546.
14. Grover TR, Asikainen TM, Kinsella JP, Abman SH, White CW. Hypoxia-inducible factors HIF-1α and HIF-2α are decreased in an experimental model of severe respiratory distress syndrome in preterm lambs. *Am J Physiol Lung Cell Mol Physiol* 2007;292:L1345–L1351.
15. Asikainen TM, Chang LY, Coalson JJ, Schneider BK, Waleh NS, Ikegami M, *et al.* Improved lung growth and function through hypoxia-inducible factor in primate chronic lung disease of prematurity. *FASEB J* 2006;20:1698–1700.
16. Ito R, Barnes EA, Che X, Alvira CM, Cornfield DN. SM22α cell-specific HIF stabilization mitigates hyperoxia-induced neonatal lung injury. *Am J Physiol Lung Cell Mol Physiol* 2022;323:L129–L141.
17. Hirsch K, Taglauer E, Seedorf G, Callahan C, Mandell E, White CW, *et al.* Perinatal hypoxia-inducible factor stabilization preserves lung alveolar and vascular growth in experimental bronchopulmonary dysplasia. *Am J Respir Crit Care Med* 2020;202:1146–1158.
18. Domingo-Gonzalez R, Zanini F, Che X, Liu M, Jones RC, Swift MA, *et al.* Diverse homeostatic and immunomodulatory roles of immune cells in the developing mouse lung at single cell resolution. *eLife* 2020;9: e56890.
19. Mazure NM, Chen EY, Laderoute KR, Giaccia AJ. Induction of vascular endothelial growth factor by hypoxia is modulated by a phosphatidylinositol 3-kinase/Akt signaling pathway in Ha-ras-transformed cells through a hypoxia inducible factor-1 transcriptional element. *Blood* 1997;90:3322–3331.
20. Semenza GL. Vasculogenesis, angiogenesis, and arteriogenesis: mechanisms of blood vessel formation and remodeling. *J Cell Biochem* 2007;102:840–847.
21. Yu AY, Frid MG, Shimoda LA, Wiener CM, Stenmark K, Semenza GL. Temporal, spatial, and oxygen-regulated expression of hypoxia-inducible factor-1 in the lung. *Am J Physiol* 1998;275:L818–L826.
22. Iyer NV, Kotch LE, Agani F, Leung SW, Laughner E, Wenger RH, *et al.* Cellular and developmental control of O_2 homeostasis by hypoxia-inducible factor 1 alpha. *Genes Dev* 1998;12:149–162.
23. Brusselmans K, Compernolle V, Tjwa M, Wiesener MS, Maxwell PH, Collen D, *et al.* Heterozygous deficiency of hypoxia-inducible factor-2α protects mice against pulmonary hypertension and right ventricular dysfunction during prolonged hypoxia. *J Clin Invest* 2003;111:1519–1527.
24. Vadivel A, Alphonse RS, Etches N, van Haaften T, Collins JJ, O'Reilly M, *et al.* Hypoxia-inducible factors promote alveolar development and regeneration. *Am J Respir Cell Mol Biol* 2014;50:96–105.
25. Saini Y, Harkema JR, LaPres JJ. HIF1α is essential for normal intrauterine differentiation of alveolar epithelium and surfactant production in the newborn lung of mice. *J Biol Chem* 2008;283: 33650–33657.
26. Dai Z, Li M, Wharton J, Zhu MM, Zhao YY. Prolyl-4 hydroxylase 2 (PHD2) deficiency in endothelial cells and hematopoietic cells induces obliterative vascular remodeling and severe pulmonary arterial hypertension in mice and humans through hypoxia-inducible factor-2α. *Circulation* 2016;133:2447–2458.
27. Kapitsinou PP, Rajendran G, Astleford L, Michael M, Schonfeld MP, Fields T, *et al.* The endothelial prolyl-4-hydroxylase domain 2/hypoxia-inducible factor 2 axis regulates pulmonary artery pressure in mice. *Mol Cell Biol* 2016;36:1584–1594.
28. Assali NS, Kirschbaum TH, Dilts PV. Effects of hyperbaric oxygen on uteroplacental and fetal circulation. *Circ Res* 1968;22:573–588.
29. Herriges M, Morrisey EE. Lung development: orchestrating the generation and regeneration of a complex organ. *Development* 2014; 141:502–513.
30. Kim YM, Barnes EA, Alvira CM, Ying L, Reddy S, Cornfield DN. Hypoxia-inducible factor-1α in pulmonary artery smooth muscle cells lowers vascular tone by decreasing myosin light chain phosphorylation. *Circ Res* 2013;112:1230–1233.
31. LaGory EL, Giaccia AJ. The ever-expanding role of HIF in tumour and stromal biology. *Nat Cell Biol* 2016;18:356–365.
32. De Paepe ME, Mao Q, Powell J, Rubin SE, DeKoninck P, Appel N, *et al.* Growth of pulmonary microvasculature in ventilated preterm infants. *Am J Respir Crit Care Med* 2006;173:204–211.
33. Boström H, Willetts K, Pekny M, Levéen P, Lindahl P, Hedstrand H, *et al.* PDGF-A signaling is a critical event in lung alveolar myofibroblast development and alveogenesis. *Cell* 1996;85:863–873.
34. Vaccaro C, Brody JS. Ultrastructure of developing alveoli. I. The role of the interstitial fibroblast. *Anat Rec* 1978;192:467–479.
35. Dai CX, Gao Q, Qiu SJ, Ju MJ, Cai MY, Xu YF, *et al.* Hypoxia-inducible factor-1α, in association with inflammation, angiogenesis and MYC, is a critical prognostic factor in patients with HCC after surgery. *BMC Cancer* 2009;9:418.
36. Pedeutour-Braccini Z, Burel-Vandenbos F, Gozé C, Roger C, Bazin A, Costes-Martineau V, *et al.* Microfoci of malignant progression in diffuse low-grade gliomas: towards the creation of an intermediate grade in glioma classification? *Virchows Arch* 2015;466:433–444.
37. Gale NW, Thurston G, Hackett SF, Renard R, Wang Q, McClain J, *et al.* Angiopoietin-2 is required for postnatal angiogenesis and lymphatic patterning, and only the latter role is rescued by angiopoietin-1. *Dev Cell* 2002;3:411–423.
38. Thébaud B, Goss KN, Laughon M, Whitsett JA, Abman SH, Steinhorn RH, *et al.* Bronchopulmonary dysplasia. *Nat Rev Dis Primers* 2019;5:78.
39. Aghai ZH, Faqiri S, Saslow JG, Nakhla T, Farhath S, Kumar A, *et al.* Angiopoietin 2 concentrations in infants developing bronchopulmonary dysplasia: attenuation by dexamethasone. *J Perinatol* 2008;28: 149–155.
40. Felcht M, Luck R, Schering A, Seidel P, Srivastava K, Hu J, *et al.* Angiopoietin-2 differentially regulates angiogenesis through TIE2 and integrin signaling. *J Clin Invest* 2012;122:1991–2005.
41. Reiss Y, Droste J, Heil M, Tribulova S, Schmidt MHH, Schaper W, *et al.* Angiopoietin-2 impairs revascularization after limb ischemia. *Circ Res* 2007;101:88–96.
42. Randi AM, Smith KE, Castaman G. von Willebrand factor regulation of blood vessel formation. *Blood* 2018;132:132–140.
43. Holash J, Maisonpierre PC, Compton D, Boland P, Alexander CR, Zagzag D, *et al.* Vessel cooption, regression, and growth in tumors mediated by angiopoietins and VEGF. *Science* 1999;284:1994–1998.
44. Ivan M, Haberberger T, Gervasi DC, Michelson KS, Günzler V, Kondo K, *et al.* Biochemical purification and pharmacological inhibition of a mammalian prolyl hydroxylase acting on hypoxia-inducible factor. *Proc Natl Acad Sci USA* 2002;99:13459–13464.
45. Steffes LC, Froistad AA, Andruska A, Boehm M, McGlynn M, Zhang F, *et al.* A Notch3-marked subpopulation of vascular smooth muscle cells is the cell of origin for occlusive pulmonary vascular lesions. *Circulation* 2020;142:1545–1561.